

Figure 3.67: Missing Mass resolution (σ) as a function of the relative momentum resolution and absolute angular resolution (left panel). Missing mass reconstruction for $e + p \rightarrow e' + K^+ + Y$ (right panel).

- Neutral particle identification. Some of the reaction channels studied can benefit from the direct detection of neutral (γ , n , etc.) particles. Even partial information (i.e. direction) might be usable in selected cases.

The requirements listed above are common to the strangeness GPD studies described elsewhere in this document. These experiments will benefit if additional particle identification information is available, especially for K^+ .

3.7 Electroproduction at very small Q^2

3.7.1 Introduction

The current photoproduction setup of CLAS, producing real bremsstrahlung photons tagged by a magnet spectrometer for the scattered electrons, can not be operated at 11 GeV energies. Instead, we are planning to use quasi-real photons produced when electrons are scattered at very forward angles (*i.e.*, scattering angles about 1°). Electron scattering at very small angles, with coincidence detection of hadronic final states, is a very attractive alternative to photoproduction experiments. We plan to use a small angle forward electron tagger in coincidence with the detection of multi-particle final states at the CLAS⁺⁺ detector to study electroproduction at Q^2 values of about 10^{-2} GeV². Electroproduction at these very small values of Q^2 using unpolarized electrons is equivalent to photoproduction using partially linearly polarized photons [206].

The physics program using this facility will take advantage of polarized photons with relatively high photon fluxes. Since electrons are tagged after their target inter-

actions, this technique allows the use of high electron currents, and permits to achieve high luminosity on thin targets (*i.e.*, gas targets with target recoil detection capabilities) at CLAS⁺⁺. Knowledge of the photon linear polarization, together with the use of the nearly 4π coverage for hadronic final states of CLAS⁺⁺, will allow the study of meson spectroscopy in a competitive and complementary experimental environment to the already planned coherent bremsstrahlung production experiments.

There are many physics topics that can take advantage of these beam and detector characteristics,

- meson spectroscopy (especially the study of high mass states, consisting of ordinary mesons, hybrids, and mesons with exotic J^{PC}) using H₂ and ⁴He targets,
- wide-angle pion Compton scattering,
- time-like Compton scattering,
- J/ψ production near threshold,
- high- t physics,
- study of parton distributions at low Q^2 ,
- low x_{Bj} physics (shadowing) on heavy targets,
- high mass baryon production, *e.g.*, Ξ baryons.

Kinematics, rates, and backgrounds for this facility are briefly described in the next section. The physics program of the first two items in the list are then described in detail. The third item in the list, time-like Compton scattering, has been described previously in the DVCS section. No detailed discussion of the other topics will be given.

Kinematics and Rates

The kinematic range covered by such a facility, for 11 GeV incoming electrons, is shown in table 3.3. Figure 3.68 shows total electroproduction rates expected in our kinematic range assuming a luminosity of 10^{34} cm⁻²sec⁻¹. The total inclusive electron rate in the low Q^2 detector will be of about 10 kHz (for $\nu=8$ to 9 GeV).

Electron scattering contains contributions from one-photon exchange (Born process), from QED vacuum polarization loops, and from the emission of additional real photons (radiative corrections). The importance of the internal radiative corrections in relation to the Born process depends on the kinematics. Radiative corrections increase with decreasing Q^2 and increasing ν . We have used the program RADGEN 1.0 [207] to calculate the contributions of internal radiative corrections to the total inclusive cross section. Figure 3.68 shows the ratio of the inelastic (Born) and elastic-radiative tails to the total inclusive cross section versus scattered electron energies.

$E_{scattered}$	1 - 4 GeV
θ	$0.5^\circ - 1.2^\circ$
ϕ	$0^\circ - 360^\circ$
ν	7 - 10 GeV
Q^2	0.003 - 0.029 GeV ²
W	3.9 - 4.6 GeV
x_{Bj}	0.0001 - 0.002

Table 3.3: Kinematic range covered by the low Q^2 tagger.

Inelastic processes represent about 4% of the total cross section in our kinematic range. It is, therefore, essential for our measurements to require a tight trigger coincidence between the forward tagger and the detection of multi-particle final states in the CLAS detector. The total rate of inelastic events is, therefore, expected to be about 400 Hz (for $\nu=8$ to 9 GeV).

Backgrounds to the very forward electron tagger include bremsstrahlung and Møller processes. Bremsstrahlung photon production peaks at very forward angles (about $\delta\theta \approx m_e/E$), therefore their contribution at angles $\theta > 0.5^\circ$ is very small. We have calculated the Møller electron rates at forward angles. Figure 3.69 shows the angular distribution of Møller electrons for an electron luminosity of $10^{34} \text{ cm}^{-2} \text{ sec}^{-1}$. The rates of Møller electrons show a minimum about 0.5° to 1.4° , which correspond to our tagging angles. These backgrounds have been checked using a GEANT-3 simulations. Most of the background comes from Møller electrons. Hadronic backgrounds are about two order of magnitude smaller. The total expected background is about 6 MHz. This background can be almost totally rejected at the trigger level by energy and clustering thresholds in the low Q^2 detector.

Virtual (‘almost real’) photoproduction presents several advantages over photon bremsstrahlung beams. Only electrons corresponding to photons that have produced hadronic interactions are registered by the tagger, thus allowing a higher beam flux for a comparable accidental rates. This is a major advantage for using thin targets. For “post-tagged”, very low Q^2 , beams the tagged electron flux is proportional to the hadronic rate and not to the incoming photon flux, so that the photon flux is not limited by the electron tagging rate. It is, therefore, possible to run higher beam currents into thin targets without an increase in accidental rates. As a consequence, higher luminosities can be achieved using thin (in gm/cm^2) targets than in case of a tagged bremsstrahlung beam.

As discussed earlier, for a luminosity of $10^{34} \text{ cm}^{-2} \text{ sec}^{-1}$ the total tagged electron rate will be of order 6 MHz, producing an inelastic signal of about 400 Hz. To be able to reduce those total electron rates, a selective trigger and tight coincidence window between the low Q^2 tagger signal and a multi-particle signal in CLAS⁺⁺ needs to be achieved. Møller background will produce two clusters containing the full energy

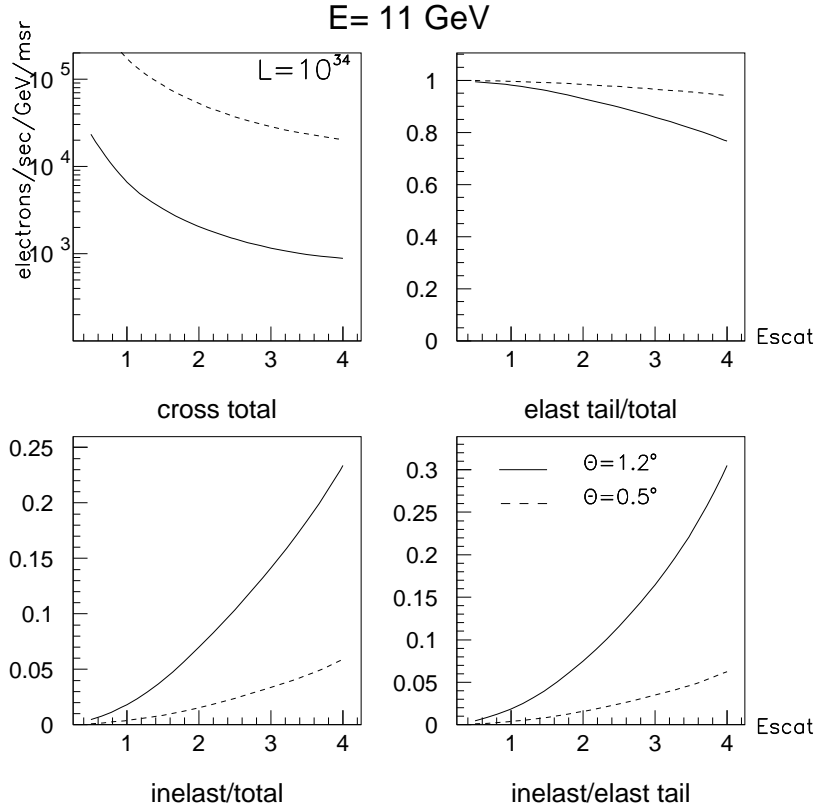


Figure 3.68: Total electroproduction rates at 11 GeV beam energy.

of the beam, instead the signal will produce one cluster with an energy of around 1 to 4 GeV. For a three prong event in CLAS⁺⁺ and energy thresholds in the low Q^2 electron detector, the data acquisition rate will be reduced to a few kHz.

The low Q^2 post-CLAS detector is currently being designed and is expected to be in operation well before the 12 GeV upgrade. Electrons undergoing small angle scattering in the CLAS target will be detected by a downstream spectrometer (about 10 meters downstream of the target) that measures the angles θ , ϕ and the electron energy. The spectrometer will consist of high rate multi-wire proportional chamber, scintillating fibers or traditional drift chamber to measure θ and ϕ of the electrons. The energy will be determined either by using a magnetic spectrometer or by a high resolution highly segmented calorimeter. We expect to achieve virtual photon energy resolution on the order of $\delta(E_\nu)/E_\nu < 0.5\%$.

3.7.2 Meson Spectroscopy on LH_2 Targets

A complete mapping of meson resonances in the mass region of 1 to 3 GeV will be particularly important for a better understanding of the QCD confinement mechanism.

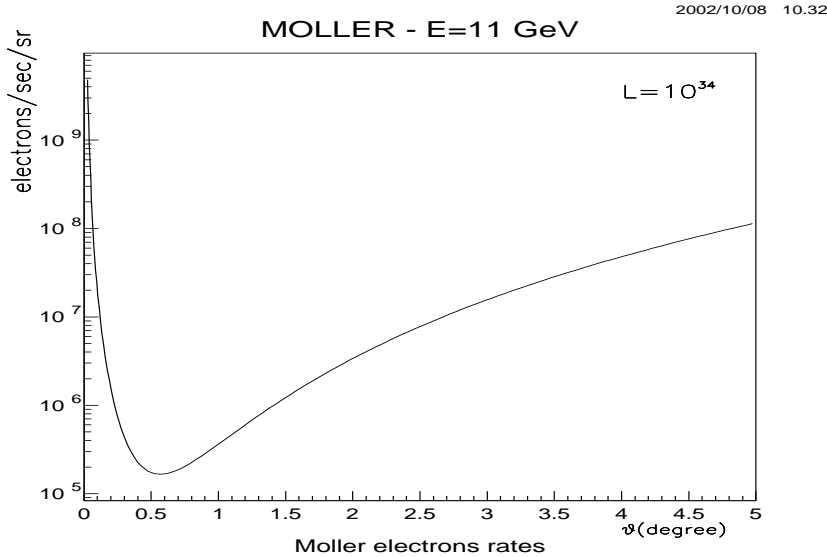


Figure 3.69: Møller electron rates

QCD predicts the existence of several new types of states beyond the naive quark model: glueballs, hybrids, multi-quark $q\bar{q}q\bar{q}$ states [208, 209]. Gluons play a central role in strongly interacting matter – quark confinement is due to gluonic forces. The clearest most fundamental experimental signature for the presence of dynamics of gluon degrees of freedom is the spectrum of gluonic excitations of hadrons. Gluonic excitations of mesons with “exotic” quantum numbers, *i.e.*, quantum numbers not accessible to the $q\bar{q}$ system, would be the most direct evidence for these states. Determining the properties of such states would shed light on the underlying dynamics of quark confinement.

The identification of these states has been difficult, as high mass resonances are generally broad and overlapping, and often have similar quantum numbers (mixing). Hadronic cross-sections are low, so statistics have been limited. Ideally, for a complete mapping of the mesons in this mass region, we will need to study each resonance through as many decay channels and production mechanisms as possible in order to disentangle mixing. To determine meson quantum numbers we use partial wave analysis (PWA) (in a broad sense, fits to the angular distributions of final states). A complete PWA requires high event statistics, as well as high resolution and geometrical detector acceptance. Meson spectroscopy at the upgraded CLAS, using the low Q^2 tagger, will fulfill many of those stipulations. The general idea of PWA is to parameterize the intensity distribution in the space of quantum numbers available to the observed final states. The intensity distribution is written as a sum of interfering and non-interfering amplitudes (partial waves), for example in the reflectivity basis [210]: $I(\tau) = \sum_{\epsilon,k} |\sum_b^\epsilon V_{bk}^\epsilon A_b(\tau)|^2$. The variable k is the rank of the fit, related to the set of partial waves from the production vertex, τ describes the set of angular

distributions that define the decays, and b is an index for the set of quantum number accessible to the final state system. The spin density matrix will define the rank of the production waves, entering the production amplitude V_{bk} . The decay amplitudes, $A_b(\tau)$, are given by geometrical terms of combinations of Clebsch-Gordan coefficients (D functions). A maximum likelihood fit is done to the intensity distribution by a set of given partial waves and reasonable assumptions of the production mechanisms. The goodness of the fit is related to the statistics (number of events per binned data) and the rank of the matrix, number of parameters to be fitted. The fit could then be improved by using higher statistics or (equivalently) by reducing the rank of the fit by having more information about the production mechanisms.

The knowledge of photon polarization simplifies the PWA by giving direct information on the production mechanisms and therefore reducing the rank of the fit. Electroproduction at these very small values of Q^2 using unpolarized electrons *is equivalent to photoproduction using partially linearly polarized photons*. The matrix element for the electron scattering process in the one-photon exchange is:

$$|\mathcal{M}|^2 = (2e^4/Q^2)T_{\mu\nu}L^{\mu\nu}$$

where $T_{\mu\nu}$ is the hadronic tensor (expressed in terms of nucleon structure functions) and $L^{\mu\nu}$ is the virtual photon polarization density matrix. Defining the photon polarization as:

$$\epsilon = [1 + 2\frac{(Q^2 + \nu^2)}{Q^2} \tan^2(\theta/2)]^{-1},$$

and the longitudinal polarization $\epsilon_L = \frac{Q^2}{\nu^2}\epsilon$, the polarization density matrix can be written as [206]:

$$\begin{pmatrix} \frac{1}{2}(1 + \epsilon) & 0 & -[\frac{1}{2}\epsilon_L(1 + \epsilon)]^{1/2} \\ 0 & \frac{1}{2}(1 - \epsilon) & 0 \\ -[\frac{1}{2}\epsilon_L(1 + \epsilon)]^{1/2} & 0 & \epsilon_L \end{pmatrix}$$

At very low values of Q^2 the virtual photon beam becomes, for all practical purposes, almost a real photon beam, since

$$\epsilon_L = \frac{Q^2}{\nu^2}\epsilon = 10^{-3}\epsilon \approx 0.$$

Since there is no longitudinal contribution, the matrix represents the spin density matrix of real (transverse) photons.

Figure 3.70 shows the values of the photon polarization in our kinematic range. The photon polarization produced by an 11 GeV electron beam ranges between 65% (7 GeV photons) to 20% (10 GeV photons). Since the polarization is measured for

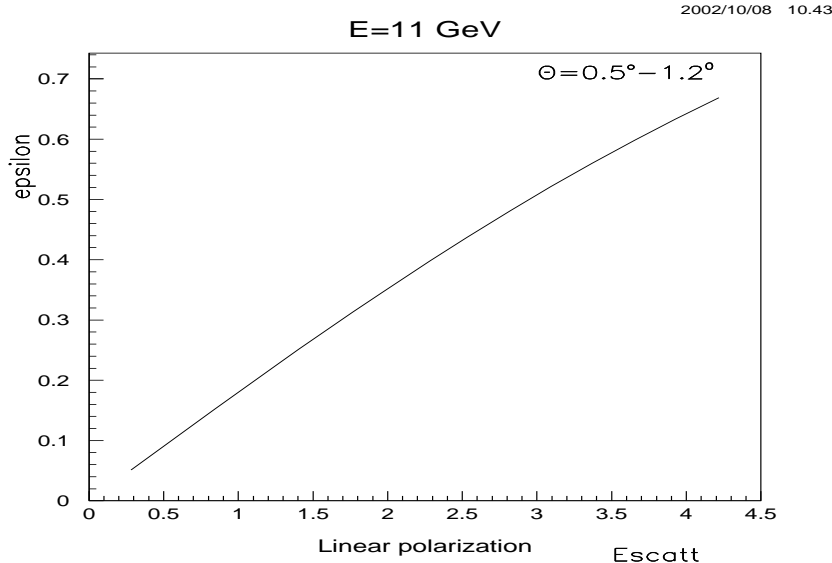


Figure 3.70: Virtual Photon Polarization

each photon, in a sense, all of the photons in the beam are polarized. In contrast, the polarization produced by coherent bremsstrahlung beams is a strong function of the energy of the bremsstrahlung photons.

To illustrate the importance of linear polarization, a simulation of meson production via photoproduction physics was performed (for an electron beam energy of 6 GeV). Events were generated according to t channel phase space with a $\frac{\partial\sigma}{\partial t} \propto e^{5t}$. These events were weighted according to a photoproduction cross-section as a function of polarization and with a one pion exchange production (OPE) mechanism. Included in the description of the cross-section were 4 resonances: $a_1(1260)$, $a_2(1320)$, $\pi_1(1600)$ and $\pi_2(1670)$. Events were then filtered through a *current CLAS geometric acceptance simulation (GSIM)*. The events were simulated for $\nu = 4$ GeV, so the polarization of the virtual photon was $\approx 60\%$ (similar to the one expected in the upgrade).

The effects of polarization can be directly seen in Figure 3.71. Because pion exchange corresponds to unnatural parity exchange the ϕ dependence of the produced 3π system will flip depending on the naturality of the state [211]. These two figures differ only in the direction of the photon polarization and correspond to the two eigenstates of reflectivity. In Figure 3.71 (a) are those events where the photon polarization is normal to the production plane, and (b) are those events where the photon polarization is in the production plane. Due to parity conservation in the production process, states of the same reflectivity but opposite naturality will have opposite ϕ distributions, which may be observed in the figure. It is most clearly seen for the band at the $a_2(1320)$ mass. This distribution is $\cos^2(\phi)$ in one figure and $\sin^2(\phi)$ in the other. Another band at a mass near 1.7 GeV has the opposite ϕ behavior of the $a_2(1320)$. It corresponds to the $\pi_2(1670)$ which has a naturality

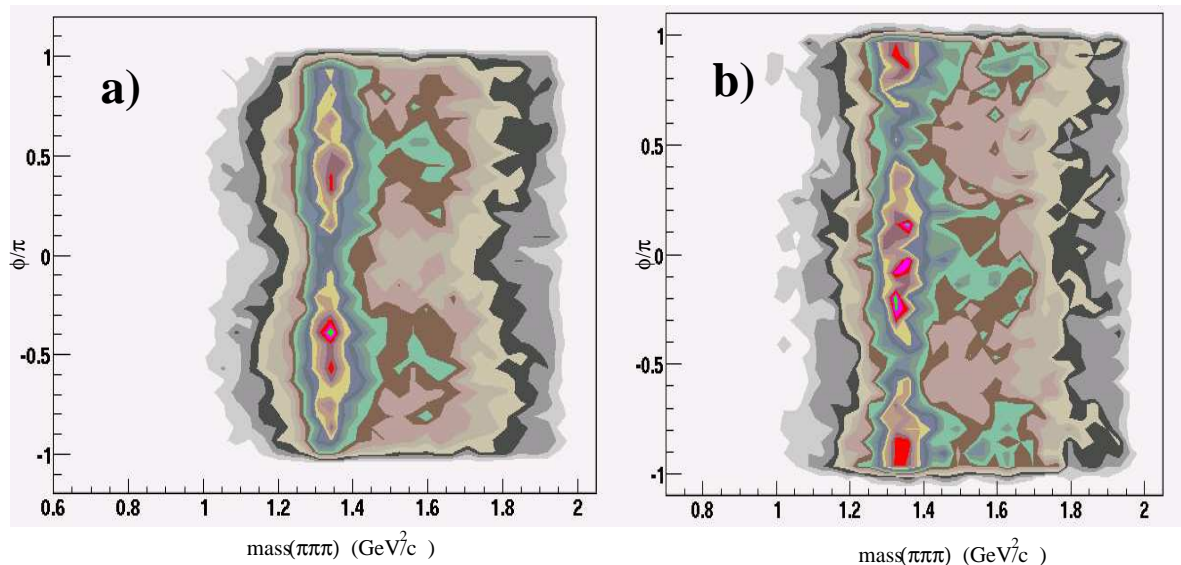


Figure 3.71: The ϕ/π vs $\text{Mass}[3\pi]$ for those events with the polarization in the production plane. The simulated polarization was set to 60%.

opposite that of the $a_2(1320)$.

In practice, the spin-parity, and therefore the naturality, of a resonance is measured via a partial wave analysis. Using this and the known beam polarization in formation, the naturality of the unknown exchange particle can be determined thus providing key insight into the production mechanism.

Spectroscopy studies of mesons have started at JLab with CLAS at lower energies [212]. Preliminary results of these experiments show the viability of such studies using the current CLAS configuration. PWA of simple final states ($\pi\pi$) have already been carried out successfully using current CLAS data. CLAS experiment E01-017 studied the reaction $\gamma p \rightarrow p\pi^+\pi^-$. For the purpose of this study, we have chosen exclusive final states where a π^+ , a π^- , and a proton are detected in CLAS. The $\pi^+\pi^-$ invariant mass distribution shows a clear signal at the mass of the ρ and the f_2 . The results of a preliminary PWA of the system is shown in Figure 3.72. The ρ meson is identified as a $J^{PC} = 1^{--}$ state, while s-channel helicity conservation is clearly observed, as the ρ signal is dominated by the $|J_z| = 1$ partial wave. There is also some leakage from the $J^{PC} = 2^{++}$ $f_2(1270)$ partial wave into the 1^{--} wave as observed in Figure 3.72, in the 1^{--} partial wave intensity in the 1.1 to 1.2 mass range. Since the final state is composed of two identical pseudoscalars, there are also purely mathematical ambiguous solutions that at this moment, we have not accounted for but have plans to incorporate as the analysis matures. These ambiguities will be mostly resolved when using linearly polarized photons and larger acceptances.

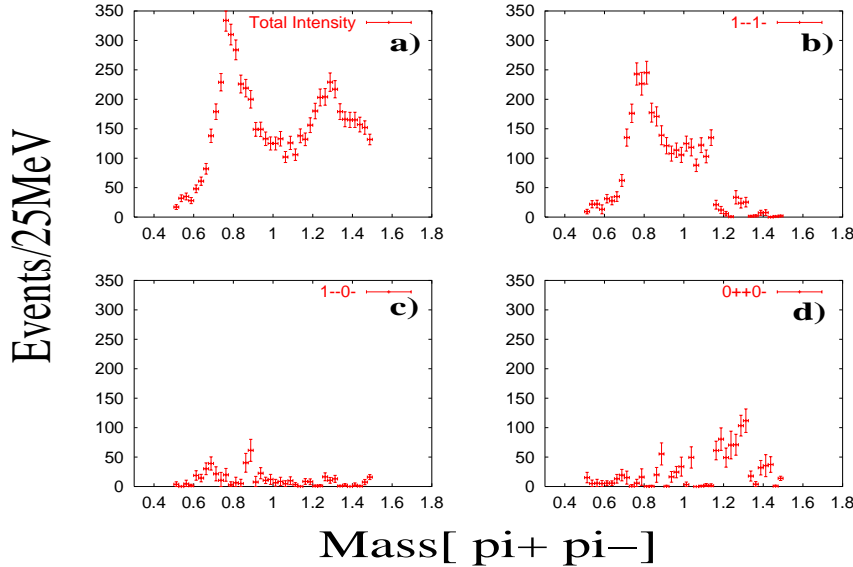


Figure 3.72: CLAS E01-017 preliminary partial wave analysis results of the reaction $\gamma p \rightarrow p\pi^+\pi^-$. (a) Total intensity distribution. (b) Intensity for the $J^{PC} = 1^{--}, |J_z| = 1$ wave. (c) Intensity for the $J^{PC} = 1^{--}, |J_z| = 0$ wave. (d) Intensity for the $J^{PC} = 0^{++}$ wave.

Even if events are not fully measured over the entire solid angle, hermiticity will provide information to veto events that are not fully reconstructed, reducing leakages among different waves due to poorly reconstructed events. CLAS⁺⁺ will be able to measure multi-charged and multi-photon particle final states with good acceptances for up to four or five final state particles. PWA of more than four or five final particles becomes difficult and increasingly unreliable, limiting the possible number of decay channels to be analyzed. We plan to obtain the high statistics that will be needed to access channels with four observed particles in the final state by running high beam currents. The rate at which we will be able to obtain data will likely be determined by limits of our DAQ system. In comparison, current CLAS experiments using CLAS bremsstrahlung beams at DAQ rates of 2 KHz were able to achieve comparable statistics (in three particles final states) to previous π beam experiments in about one or two months (“real time”) of running.

Another important meson spectroscopy study is of strangeonia. Strangeonia are mesons made of dominantly (valence dominance) $s\bar{s}$ unflavored strange quarkonia. They are associated with the radial and orbital excited states of the $\phi(1020)$ meson, that is known to be composed mainly of $s\bar{s}$ valence quarks. We will study strangeonium states with masses ranging from 1 up to about 2.5 GeV. Given that strangeonium states have intermediate masses between the light (up, down) and heavy (charm, bottom) quarkonia, they are very useful in the study of the QCD confinement potential in the transition region from short to large distance behavior. Particularly,

$s\bar{s}$ excitations provide a range of quark separations where the confinement potential can be explored from the perturbative to the non-perturbative regimes. This character has been pointed out by Gell-Mann and recently by Barnes, Page and Black [213]: “the similarity between the $s\bar{s}$ spectrum, the light meson $n\bar{n}$ and the heavy $Q\bar{Q}$ systems needs to be understood to bridge the gap between Heavy Quark Effective Theory (HQET) and the light quark world in which we live”. Strangeonia are poorly understood – of the 22 strangeonium states expected below a mass of 2.2 GeV, only 5 are well identified. The clarification of the strangeonium spectra in this mass range is an important and necessary step for the advance of intermediate mass meson spectroscopy.

3.7.3 Meson Spectroscopy Using Coherent Production on ${}^4\text{He}$.

Partial wave analysis is a key element in any meson spectroscopy experiment. Use of a linearly polarized photon beam is one way to reduce the number of parameters in the PWA, and therefore reduce the ambiguities and the required statistics. Another way of simplifying the PWA is the selection of a production mechanism that reduces the number of allowed helicity states and/or allowed exchange particles. Such processes can be coherent production of t -channel meson on nuclei. Particularly, coherent production of mesonic states on ${}^4\text{He}$, where the target nucleus remains intact after the interaction, has several advantages for the PWA. These are due to the spin-0 and isospin-0 of ${}^4\text{He}$. This type of reaction is a powerful tool for studying neutral mesons.

Examples of such reactions can be coherent production of $\pi\eta$ and $\pi\eta'$ final states on a ${}^4\text{He}$ target. The attractive feature of these final states is that in P -wave these are $J^{PC} = 1^{-+}$ exotics. Photoproduction of $\pi\eta$ and $\pi\eta'$ on the nucleon proceeds only via C-odd ρ or ω exchanges. Since ${}^4\text{He}$ has isospin-0, only ω exchange is allowed. Due to spin-0 of ${}^4\text{He}$, the helicity of the final state in forward production should be equal to the helicity of the incoming photon, which means that S wave production in the final state is not allowed, and the sum over the helicity of the final state will be reduced to one term. **The key feature of these measurements is that the recoiling helium nuclei remains intact. This requires direct detection of the recoiling ${}^4\text{He}$ nucleus.**

PWA formalism

In photoproduction (as in the case of pion beams) the mechanism leading to natural parity and unnatural parity exchange (NPE and UPE) in the t -channel do not interfere and contribute to different amplitudes with different angular dependences. If the production mechanism is defined, it provides additional constraints for the PWA.

Differential cross section of t -channel meson photoproduction in the rest frame of

the produced state (Gottfried-Jackson frame) can be written as⁶:

$$\frac{d\sigma}{d\Omega} = |A_0 + A_-|^2 + |A_+|^2. \quad (3.60)$$

Here A_0 and A_- are the helicity amplitudes for the UPE, and A_+ is for NPE. The complete expression for helicity amplitudes can be found in [214] and references therein.

In the case of coherent photoproduction of $\pi\eta(\pi\eta')$ on ${}^4\text{He}$, when only ω exchange is allowed, A_0 and A_- will vanish and only A_+ contributes. Moreover, production of a state with $L = 0$ is forbidden due to helicity conservation in the S-channel (SCHC)⁷, and the helicity of the $\pi\eta$ ($\pi\eta'$) system should be that of the incoming photon. Therefore, A_+ can be written as:

$$A_+ = \sum_{L=1}^{L_{max}} (2L+1)^{1/2} \sqrt{2} L_{1+} \text{Im}(D_{10}^L(\Theta, \phi)), \quad (3.61)$$

where L is the total angular momentum of $\pi\eta$ ($\pi\eta'$) system, and the sum is taken up to the highest possible angular momentum of the produced pair in the given mass range. $L_{\lambda+}$ is the amplitude for the production of $\pi\eta$ ($\pi\eta'$) with spin L via NPE. These amplitudes are the parameters in the PWA. The angular distribution of the decay meson will be analyzed in each energy bin to determine the production strength of a particular wave.

The function $D_{\lambda_0}^L(\Theta, \phi)$ defines the angular distribution of the π (or η/η') in the Gottfried-Jackson frame. Θ and ϕ are polar and azimuthal angles of the meson in that frame. Using the standard form for $D_{10}^L(\Theta, \phi)$ the differential cross section for the production of interfering waves with $L \leq 3$ can be written as:

$$\begin{aligned} \frac{d\sigma}{d\Omega} &= | -\sqrt{3}P_{1+} \sin(\phi) \\ &+ -\sqrt{15}D_{1+} \sin(\phi) \cos(\Theta) \\ &+ -\frac{\sqrt{15}}{2}F_{1+} \sin(\phi)(5 \cos^2(\Theta) - 1) |^2, \end{aligned} \quad (3.62)$$

It should be noted that the cross section is proportional to $\sin^2(\phi)$, which is due to the assumption of SCHC. The measured angular dependence will be an independent test of this assumption. In the PWA only three mass-dependent parameters, P_{1+} , D_{1+} and F_{1+} , need to be determined.

⁶Here and in the following we will use notations from Ref.[214].

⁷This is valid at our kinematics where $\frac{\sqrt{-(t-t_{min})}}{E_\gamma} \sim 0$

Experimental issues

CLAS⁺⁺ will have large coverage for neutral and charged particles in the forward direction and nearly 2π coverage at scattering angles $\theta > 45^\circ$. The detection of a multiparticle final state from many-body decays of final state mesons can therefore be accomplished. The main issue in these measurements will be the detection of the recoiling ${}^4\text{He}$ nuclei.

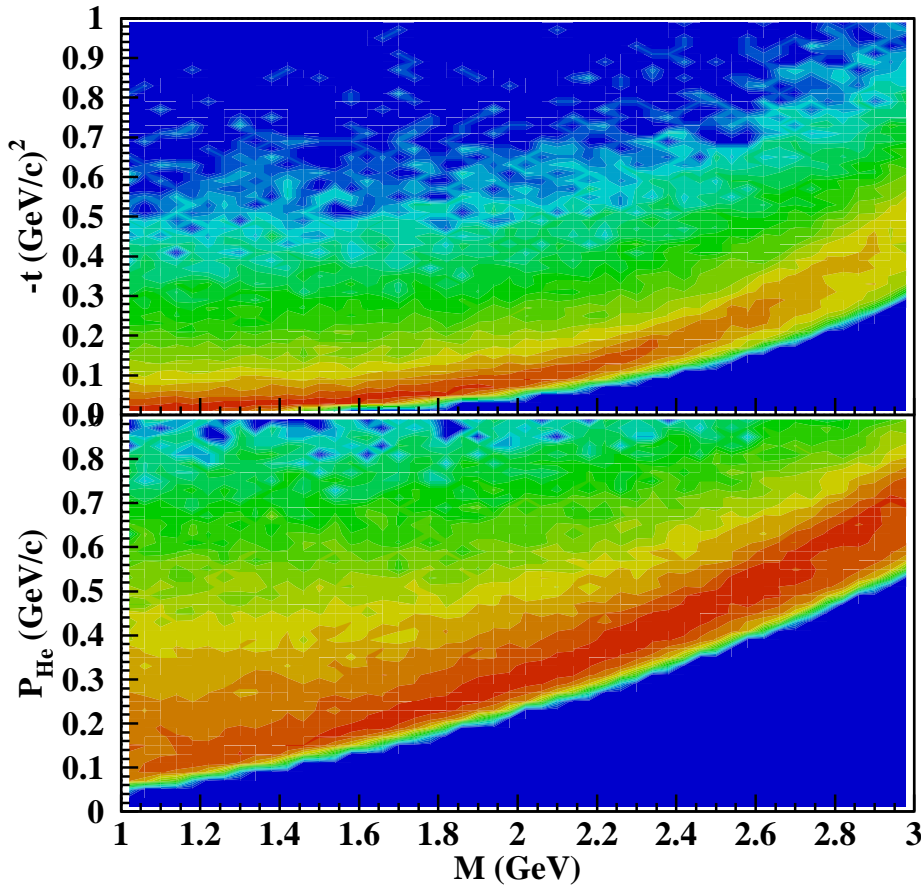


Figure 3.73: Kinematics of proposed measurements. Top plot - four momentum transferred squared as function of the produced t -channel meson mass. The lower edge corresponds to t_{min} for a maximum photon energy of 9 GeV. The lower plot shows the corresponding momentum distribution of recoiling ${}^4\text{He}$ nuclei.

For reasonable production rates, measurements should be carried out at small momentum transferred, close to t_{min} , to limit the cross section reduction due to the ${}^4\text{He}$ form factor. This implies that recoiling target nuclei will have very small momenta, as shown in Figure 3.73. For a mass range $M < 2.5 \text{ GeV}/c^2$ the momentum of the recoiling nucleus is $\leq 0.35 \text{ GeV}/c$. ${}^4\text{He}$ nuclei with such low momenta will not

be able to pass through any size liquid target. A lighter target, e.g. using pressurized gas, is needed. Using a gas target with the conventional photon tagging method is not an option due to severe luminosity limitations. **Electron scattering at small angles opens up a very attractive alternative to conduct experiments on “thin” targets.**

Use of an electron beam has many advantages: the small size of a few hundred μm high precision electron beam will allow use of a small diameter target cell. This will help reduce the thickness of the target walls at a given pressure (density), and therefore reduce the amount of the material in the way of final state particles. Also a small size electron beam will allow better determination of the interaction point in the plane perpendicular to the direction of the beam. For the required luminosity, the density of the target and the beam current can be varied without compromising the signal/accidental ratio.

The proposed detector for tagging very low momentum backward going protons in electron deuteron scattering (for studying the neutron structure), will allow detection of ${}^4\text{He}$ nuclei for momenta as low as $\sim 0.25 \text{ GeV}/c$ (corresponding to a transferred momentum squared in the t -channel of $t_{thr} = 0.07 \text{ (GeV}/c)^2$). A description of the gas target and the detector for low energy protons is presented in Section ???. To use this detector for meson spectroscopy, the only change required is to replace the deuterium gas in the target cell by helium gas.

Expected rates

In this section, estimates for the production rate of exotic states in the mass range from 1.4 to 1.6 GeV in the $\pi\eta$ decay channel are presented. States with exotic quantum numbers have been reported in previous experiments. We assume that exotic waves will be produced at a rate of 10% compared to the production rate for A_2 in the same decay mode.

The cross section for t -channel meson electroproduction can be expressed as a sum of the cross sections for transversely (σ_T), and longitudinally (σ_L) polarized photons:

$$\frac{d\sigma_{eN \rightarrow eM^0N}}{dQ^2 dW dt} = \Gamma_W \cdot \left(\frac{d\sigma_T}{dt} + \epsilon \frac{d\sigma_L}{dt} \right) \quad (3.63)$$

were Γ_W is the virtual photon flux, and ϵ is the virtual photon polarization.

For the kinematics of the proposed measurements, $Q^2 \sim 0.01 \text{ (GeV}/c)^2$, σ_L can be neglected, and σ_T can be calculated using the VDM formalism from the photoproduction cross section:

$$\sigma_T = \left(\frac{m_\rho^2}{m_\rho^2 + Q^2} \right)^2 \cdot \sigma_{\gamma N \rightarrow M^0 N} \quad (3.64)$$

were m_ρ is the ρ meson mass, and $\sigma_{\gamma N \rightarrow M^0 N}$ is the photoproduction cross section.

Production on nuclei is usually used to enhance the statistics. In the proposed experiment the gain in the production rate (cross section) will be a factor of 16, however the requirement of leaving the ${}^4\text{He}$ nucleus intact will add an extra form-factor, $F_{He}(t)$, in the amplitude, and the cross section will be:

$$\frac{d\sigma_{eHe \rightarrow eM^0He}}{dQ^2 dW dt} = \Gamma_W \cdot \frac{d\sigma_{\gamma N \rightarrow M^0 N}}{dt'} \cdot (4F_{He}(t))^2 \quad (3.65)$$

For A_2 , the differential cross section can be extracted from existing experimental data ([215]). At $t' = t_{thr} - t_{min} = 0.05$ (GeV/c) 2 , we obtain $\frac{d\sigma}{dt'} \simeq 2\mu\text{b}(\text{GeV}/\text{c})^{-2}$. The proposed measurements will be carried out using a 10 cm helium gas target at 5 atm pressure. Combined with a beam of up to 500 nA a luminosity of $L = 4 \times 10^{33}$ cm $^{-2}$ sec $^{-1}$ can be achieved. Using the known branching ratios $\text{Br}(A_2 \rightarrow \pi\eta) = 14\%$ and $\text{Br}(\eta \rightarrow \gamma\gamma) = 39\%$, and the upgraded CLAS acceptance for this final state ~ 0.07 one gets 0.05 sec $^{-1}$ for the A_2 electroproduction in this channel. Assuming 10% for the ratio of an exotic wave relative to the A_2 we found 18 hour $^{-1}$ for the detection rate of an exotic in the coherent scattering of the 11 GeV electrons off a helium target.

One should note that $\pi\eta$ or $\pi\eta'$ final states are just examples of reactions that can be studied. Since CLAS $^{++}$ can operate with loose trigger requirements, all possible final states will be recorded in parallel. The spin 0 and isospin 0 of the ${}^4\text{He}$ target will give the same advantages in PWA for other final states.

3.7.4 Summary

The low Q^2 post-CLAS electron detector is currently being designed and is expected to be in operation well before the 12 GeV upgrade. Electrons that undergo small angle scattering in the CLAS $^{++}$ target will be detected by a downstream spectrometer (about 10 meters downstream of the target) that measures the angles θ , ϕ and the electron energy. The spectrometer will consist of high rate multi-wire proportional chamber, scintillating fibers or traditional drift chamber to measure θ and ϕ of the electrons. The energy will be determined either by using a toroidal magnetic spectrometer or by a high resolution highly segmented calorimeter. We expect to achieve virtual photon energy resolution on the order of $\delta(E_\nu)/E_\nu < 0.5\%$.

Virtual ('almost real') photoproduction presents complementarity to a bremsstrahlung beam. Only photons that had produced hadronic interactions are registered by the tagger, thus allowing a higher beam flux for comparable background accidentals. For "post-tagged", very low Q^2 , beams the tagged electron flux is proportional to the hadronic rate and not to the incoming photon flux, so that the photon flux is not limited by the electron tagging rate. It is therefore possible to run higher beam currents into thin targets without an increase in accidental rates.

The addition of a low Q^2 post-CLAS electron tagging detector will extend the rich physics program of CLAS $^{++}$ at 12 GeV. The meson spectroscopy program will provide measurements in a novel manner that will test models and complement measurements

made via other methods. The Wide-Angle Pion Compton Scattering and Time-like DCVS program is unique to CLAS and will add significantly to the CLAS⁺⁺ GPD physics program.